



UvA-DARE (Digital Academic Repository)

Advanced MRI in inflammatory arthritis

van der Leij, C.

[Link to publication](#)

Citation for published version (APA):

van der Leij, C. (2017). Advanced MRI in inflammatory arthritis

General rights

It is not permitted to download or to forward/distribute the text or part of it without the consent of the author(s) and/or copyright holder(s), other than for strictly personal, individual use, unless the work is under an open content license (like Creative Commons).

Disclaimer/Complaints regulations

If you believe that digital publication of certain material infringes any of your rights or (privacy) interests, please let the Library know, stating your reasons. In case of a legitimate complaint, the Library will make the material inaccessible and/or remove it from the website. Please Ask the Library: <http://uba.uva.nl/en/contact>, or a letter to: Library of the University of Amsterdam, Secretariat, Singel 425, 1012 WP Amsterdam, The Netherlands. You will be contacted as soon as possible.

Chapter 7

Characteristics of synovial inflammation in early arthritis analysed by pixel-by-pixel time-intensity curve shape analysis

Marleen G.H. van de Sande*, Christiaan van der Leij*, Cristina Lavini,
Carla A. Wijbrandts, Mario Maas, Paul P. Tak

**Both authors contributed equally*

Rheumatology 2012;51:1240-1245.

Abstract

Objective

Dynamic contrast-enhanced (DCE-MRI) time-intensity curve (TIC) shape analysis has previously been used in oncology, where fast initial enhancement and early washout are associated with malignancy. As RA synovium has some tumour-like features, we investigated DCE-MRI TIC shape expression in early arthritis in relationship to diagnosis.

Methods

Twenty-eight DMARD-naïve, early arthritis patients (<1 year) with inflammation of at least one knee joint were included. At baseline DCE-MRI of the inflamed knee joint was performed, and the TIC shape type expression, maximal enhancement, maximum slope of increase and total volume of enhancing pixels were calculated. In addition, disease activity parameters were determined. At 2 years of follow-up, patients were classified as RA or non-RA according to established classification criteria.

Results

Type 4 TIC shape, characterized by fast initial enhancement followed by a quick washout phase, was significantly higher in patients fulfilling classification criteria for RA after 2 years of follow-up compared with non-RA patients (15.6 and 7.9%, respectively, $P=0.02$). All other DCE-MRI parameters showed no differences between the groups, highlighting the specificity of this observation.

Conclusion

A high expression of aggressive DCE-MRI TIC shape Type 4 is associated with RA. Our results are consistent with the view that increased vascularity plays a key role in the pathogenesis of RA. This study underlines the rationale for further studies investigating the prospect of DCE-MRI TIC shape analysis as a diagnostic tool in early arthritis and the relationship with development of destructive disease.

Introduction

The synovium is the main affected tissue in inflammatory joint diseases: inflamed synovial tissue is characterized by hypertrophy, influx of inflammatory cells and neovascularization. Contrast-enhanced MRI is considered the gold standard for imaging synovitis^{1,2}; the contrast agent increases the synovial conspicuity and allows for visualization and volume measurements.

In dynamic contrast-enhanced (DCE)-MRI, the uptake of contrast agent in time is visualized in a time-intensity curve (TIC). The shape of this TIC is determined by tissue characteristics, such as vascularization, tissue perfusion, capillary permeability and interstitial space volume, which are influenced by the degree of inflammation.³ Computer-assisted analysis of the TIC provides quantitative assessment of synovitis. Previous studies have applied pharmacokinetic modelling and descriptive parameters, such as maximum enhancement (ME) and maximum slope of increase (MSI) to quantify synovial inflammation.⁴ The TIC shape with fast initial enhancement and early washout is associated with malignant tumours.^{5,6} Since neovascularization, increased capillary permeability and invasive growth into surrounding tissues can be seen in both malignant tumours and RA, it is conceivable that this specific TIC shape might also be associated with RA.

Recently we have developed a new technique in which TIC shape expression can be analysed pixel-by-pixel in a 3D volume.⁷ This analysis technique is less computationally demanding and at the same time more robust, as it does not make use of model assumptions or non-linear fitting compared with descriptive and pharmacokinetic analysis. Previously we have shown that Type 4 TIC shape expression, characterized by fast initial enhancement followed by early washout, appears to be increased in RA patients compared with healthy controls, thereby discriminating between inflamed and non-inflamed joints.⁸ Based on the observations in malignant tumours and the changes in vascularity in patients with arthritis, we investigated DCE-MRI TIC shape expression in early arthritis in relationship to diagnosis.

Patients and methods

Study patients

Twenty-eight patients with arthritis of at least one knee joint, who had been included in our early arthritis cohort between February 2003 and April 2006, were consecutively enrolled in the current study. All patients had arthritis duration of <12 months and were DMARD naïve. Patients were excluded if there were contraindications for (contrast-enhanced) MRI, such as claustrophobia, metal implants or elevated serum creatinine.

This study was approved by the Institutional Review Board of the Academic Medical Center and performed in accordance with the Declaration of Helsinki. All study participants gave written informed consent.

Study design

At inclusion, DCE-MRI of the inflamed knee joint (if both knees were inflamed the most inflamed joint was evaluated) was performed, and demographics and disease activity parameters were determined (as described below). The presence of IgM-RF and ACPA was measured by IgM-RF ELISA (Sanquin, Amsterdam, The Netherlands) and anti-CCP2 ELISA (Euro-Diagnostica, Arnhem, The Netherlands), respectively. At a 2-year follow-up visit, patients were classified as either RA or non-RA according to 1987 ACR RA classification criteria.⁹

Disease activity parameters

We assessed overall disease activity by the 68 tender and 66 swollen joint score, morning stiffness, patient's visual analogue scale (VAS) of global disease activity (scale 0-100 mm), ESR and CRP levels. Local disease activity of the scanned knee joint was assessed by a patient's VAS of local disease activity and pain (scale 0-100 mm). Knee joint pain and swelling were also rated by a medical examiner on a semi-quantitative scale from 0 to 3.

MRI data acquisition

MRI of the affected knee joint was performed on a 1.5 T MR-scanner (GE Signa Horizon Echospeed LX9.0, General Electric Medical Systems, Milwaukee, WI, USA) using a 3D, T1-weighted gradient echo dynamic sequence that consisted of 20 consecutive acquisitions of 20 slices with a temporal resolution of 22 s [time repetition (TR)/time echo (TE)/flip 8.1 ms/3.5 ms/30, slice thickness 4mm, field of view (FOV) 18 cm, 256-256 matrix, axial orientation]. The total imaging time of the DCE-MRI acquisition was 7 min 19 s.

Patients were placed supine with the knee joint centrally in the magnetic field in a dedicated extremity coil (quadrature detection). A 20-gauge needle infusion line was inserted, preferably in the right antecubital vein. After 60 s of initiation of the dynamic protocol, a bolus of a Gd-DTPA contrast agent (Magnevist, Schering AG, Berlin, Germany; 0.1 mmol/kg) followed by a 15 ml saline chase was delivered at an injection rate of 5 ml/s using an automatic injection device (Spectris MR Injector, MEDRAD, Warrendale, PA, USA).

DCE-MRI analysis

Images were processed using an in-house developed program¹⁰ based on Matlab software (MathWorks, Natick, MA, USA). This program analyses the time-dependent signal intensity changes of every voxel (volumetric pixel) in an imaged volume resulting in a TIC. Each TIC of every voxel is classified into one of seven predefined TIC shape categories. Every TIC shape type is associated with a colour. The TIC shape distribution of each image section is visualized in colour-coded maps^{7,8} (see also Figure 7.1) or when analysing contiguous sections in 3D parametric TIC shape volumes.⁸ In the colour parametric map, pixels with a signal below noise level are rendered in black.

All analyses were performed in a 3D volume, covering the entire synovial lining of the knee joint from the tibia plateau up to the 12th proximal slice (~5 cm). The region of interest (ROI) was manually drawn in each slice to exclude enhancing skin and muscle tissue. The non-enhancing tissue (e.g. bone and cartilage) within the ROIs is ignored by the analysis software, which leaves the enhancing synovial tissue and vascular structures within the ROI for analysis.

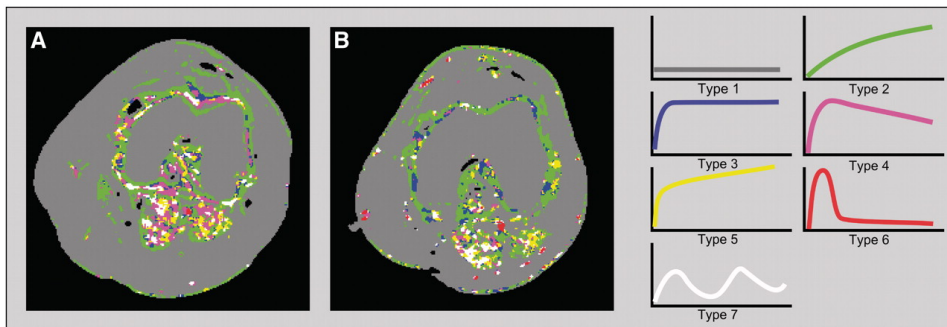


Figure 7.1 TIC shape maps (one image slice) of the knee joint of an RA patient (A) and a non-RA patient (B). The maps show marked enhancement of the synovial tissue with mainly Types 3 and 4 TIC shapes in the RA patient and mainly Types 2 and 3 TIC shapes in the non-RA patient. Types of TIC shapes shown on the right side. Type 1: no enhancement; Type 2: gradual increase of enhancement; Types 3, 4 and 5: fast initial enhancement followed by, respectively, a plateau phase, an early washout phase, sustained late enhancement; Type 6: arterial enhancement; and Type 7: all others. Pixels in which the signal is below noise level are rendered in black.

The total number of enhancing pixels was calculated and the percentage of voxels expressing each TIC shape type was calculated (percentage = number of voxels of a specific TIC shape divided by total number of enhancing voxels within the entire synovial volume). This was done to correct for differences in knee joint size between the patients. In our analysis, we only compared expression of TIC shape Types 2-5, as these types represent enhancing synovial tissue in the ROI. TIC shape Type 6 representing vessels and Type 7 representing undefined pixels [which is seen in a very

low number of pixels (median 0.3%)] were used only for the calculation of the percentage per TIC shape type.⁸ The total analysis time is 10 min per patient.

In a similar way, the image analysis program calculated the maximal enhancement (defined as the difference between maximal signal intensity and baseline, divided by signal baseline), time to peak (defined as the time between the start of enhancement and maximal signal intensity) and maximum slope of increase (defined as the largest positive signal difference between two successive acquisitions) for each voxel in the imaged volume and calculated the average values.⁸

Statistical analysis

Standard statistical software (SPSS version 16; SPSS, Chicago, IL, USA) was used for statistical analysis. Chi-square test (for categorical data) or Mann-Whitney U-test (for numerical data) was used to determine significant differences between both patient groups. Correlations between clinical parameters and DCE-MRI parameters were assessed with the Spearman's rank-order correlation coefficient. Values were expressed as percentages (female), number of positive patients (IgMRF and ACPA) or median and interquartile range (IQR). Statistical significance was defined as $P < 0.05$. As we wanted to explore parameters with a potential to be used as a discriminative marker, we did not correct for multiple testing.

Results

Disease activity and RA diagnosis

No patients were excluded based on contraindications for MRI. Of the 28 included patients, 7 patients were classified as RA and 21 patients as non-RA at 2 years of follow-up. The non-RA group consisted of patients with spondylarthritis ($n=2$), crystal arthropathy ($n=1$), HIV-related arthritis ($n=1$) and undifferentiated arthritis ($n=17$). Demographics and clinical characteristics are summarized in Table 7.1.

A significantly higher number [median (IQR)] of tender [16 (14) vs. 2 (5), $P < 0.001$] and swollen [8 (17) vs. 2 (4), $P = 0.01$] joint counts, increased CRP levels [15.0 (47.0) vs. 3.0 (5.4) mg/l, $P = 0.02$] and percentage of ACPA-positive patients ($P = 0.02$) were observed in the RA compared with the non-RA patient group. Otherwise, there were no statistically significant differences between the groups.

Table 7.1 Baseline patient characteristics.

| | All (28) | RA (7) | Non-RA (21) | P-value |
|---------------------------------------------|------------|-------------|-------------|---------|
| Female (n) | 17 | 5 | 12 | 0.56 |
| Age (years) | 47 (22) | 48 (32) | 48 (19) | 0.69 |
| 68 Tender joint count (n) | 3 (11) | 16 (14) | 2 (5) | <0.001 |
| 68 Swollen joint count (n) | 2.5 (4) | 8 (17) | 2 (4) | 0.01 |
| Patients global VAS (0-100mm) | 51 (39) | 52 (40) | 49 (40) | 0.83 |
| Morning stiffness (min) | 25 (57) | 60 (30) | 20 (52) | 0.11 |
| CRP (mg/L) | 4.8 (15.0) | 15.0 (47.0) | 3.0 (5.4) | 0.02 |
| ESR (mm/hr) | 16 (34) | 33 (39) | 14 (34) | 0.12 |
| Patients local disease activity VAS (0-100) | 42 (55) | 81 (60) | 35 (38) | 0.08 |
| Patients local pain VAS (0-100) | 37 (53) | 33 (72) | 37 (49) | 0.78 |
| Assessor local swelling (0-3) | 1 (1) | 1 (1) | 1 (1) | 0.81 |
| Assessor local pain (0-3) | 1 (1) | 1 (1) | 1 (1) | 0.12 |
| IgM rheumatoid factor positive (n) | 4 | 2 | 2 | 0.21 |
| ACPA positive (n) | 7 | 4 | 3 | 0.02 |

Medians (IQR) or percentages are shown. Mann Whitney U test or Chi-square test, whichever was appropriate was used to compare both groups. *P* values <0.05 were considered significant. VAS= visual analog scale, CRP=C-reactive protein, ESR= erythrocyte sedimentation rate.

A high percentage of Type 4 TIC shape is associated with RA

We observed a significantly higher percentage of Type 4 TIC shape (fast initial enhancement followed by a quick washout phase) in the RA patient group compared with the non-RA group [15.6% (6.6) and 7.9% (7.6), respectively, *P*=0.02] (Figure 7.2). Figure 7.1 shows examples of TIC expression in an RA patient and in a non-RA patient. Percentages of enhancement of the other three TIC shape types, ME, initial rate of enhancement and total number of enhancing pixels (representing the total volume of inflamed synovial tissue) did not show statistical differences between the two groups (Table 7.2). No significant correlations were observed between the different disease activity parameters and Type 4 TIC shape expression in the whole patient group (data not shown).

Table 7.2 DCE-MRI parameters.

| | All (n=28) | RA (n=7) | Non-RA (n=21) | P value |
|----------------------------------|---------------|---------------|---------------|---------|
| Type 2 TIC shape (%) | 61.6 (23.1) | 64.4 (14.1) | 61.5 (23.9) | 0.94 |
| Type 3 TIC shape (%) | 7.4 (11.8) | 5.0 (7.2) | 8.3 (11.5) | 0.16 |
| Type 4 TIC shape (%) | 10.6 (8.4) | 15.6 (6.6) | 7.9 (7.6) | 0.02 |
| Type 5 TIC shape (%) | 7.0 (4.9) | 7.0 (3.9) | 7.0 (5.1) | 0.35 |
| Maximal enhancement | 1.3 (0.6) | 1.2 (0.7) | 1.3 (0.6) | 0.38 |
| Initial rate of enhancement | 18.2 (10.0) | 14.3 (6.5) | 19.4 (11.2) | 0.37 |
| Total number of enhancing pixels | 37118 (23149) | 34595 (26085) | 37897 (25322) | 0.18 |

Median and IQR are shown. *P*<0.05 was considered significant. TIC= time intensity curve

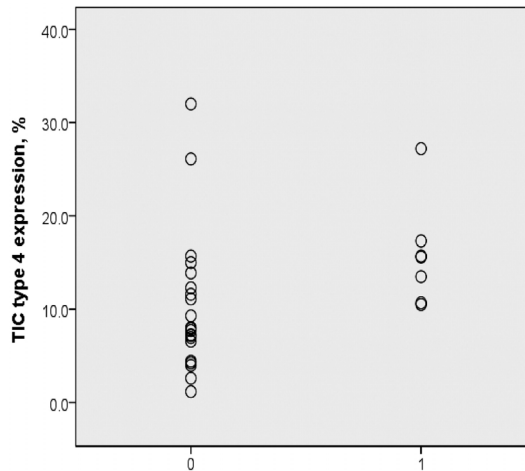


Figure 7.2 Expression of TIC type expression in non-RA (0) and RA (1) patients. TIC type is expressed as a percentage of total enhanced voxels.

Discussion

In this study we evaluated the DCE-MRI TICs in early arthritis patients. A significantly higher percentage of Type 4 TIC shape expression in RA patients compared with non-RA patients was seen, but there were no differences in the DCE-MRI descriptive parameters ME and initial rate of enhancement. This latter observation is in line with previous studies comparing RA with other types of inflammatory arthritis using descriptive DCE-MRI parameters that were similar for both groups.¹¹ Therefore, in contrast to the generally used, descriptive-only DCE-MRI analysis, the present study suggests that TIC shape analysis might have value in differentiating between RA and non-RA using DCE-MRI. However, as there was a fair overlap between the RA and non-RA patient group, the discriminative value of the Type 4 TIC needs to be studied in a larger cohort to evaluate if this analysis has additional value over standard diagnostic parameters.

In previous studies examining synovitis, DCE descriptive parameters were either calculated from a single slice or by averaging multiple slices (reviewed in⁴). This might have resulted in an over- or underestimation of the level of inflammation, as inflammation is known to be heterogeneously distributed throughout the synovial tissue. In our study we evaluated the pixel-by-pixel expression of different TIC shape types in whole synovial volume (without averaging values of separate slices), respecting the heterogeneity of inflammation within the tissue. This may be one of the reasons that TIC shape analysis enabled us to observe differences between the RA and non-RA patients, while total enhanced synovial volume was comparable between both groups.

Besides DCE-MRI, the value of static contrast-enhanced MRI parameters, such as synovial volume and bone oedema, have been studied in relationship to diagnosis and outcome. The diagnostic value of MRI parameters has been variable between various studies.¹² Although some studies have shown a clear association between the presence of bone oedema and development of erosions,¹³⁻¹⁵ the predictive value is relatively low¹² and it remains to be shown that treating RA patients based on conventional MRI findings associated with synovial inflammation and bone marrow oedema will result in better clinical outcome; therefore it is at present too early to recommend the use of MRI to guide treatment decisions.

We used in-house developed software to perform TIC shape analysis.¹⁰ This software can in principle be applied in other centres. Recently other groups have started developing similar sorts of analysis software,¹⁶ and we expect these will soon be available commercially. The Type 4 TIC shape is mostly seen in more aggressive breast tumour types and helps to differentiate benign from malignant breast tumours.^{6,17} Consistent with these findings, Type 4 TIC shape was present relatively more in patients fulfilling diagnosis of RA after 2 years of follow-up, a disease characterized by autonomous disease progression,¹⁸ which if not adequately treated, leads to joint destruction. Physiological tissue features, such as vascularization, vessel perfusion, vessel permeability and interstitial space volume, determine the shape of the TIC.^{3,19} Neovascularization and influx of inflammatory cells seen during inflammation can influence these tissue features and thereby the TIC shape. Types 3, 4 and 5 TIC are all characterized by fast initial enhancement, whereas only in TIC Type 4 is this fast enhancement followed by a quick washout phase. Vessel permeability and interstitial space volume are both known to be of significance during this washout phase²⁰ and could determine the difference between RA and non-RA patients. Type 4 TIC shape is associated with invasive growth in tumours. Conceivably, in RA TIC Type 4 expression might be related to the invasive growth, leading to the development of joint destruction. Specifically, studying TIC Type 4 expression in the synovium at sites prone to development of erosions might be of interest. Due to the relative low number of RA patients investigated, this is beyond the scope of the present study. As studies on treatment effect are still ongoing, it remains to be shown if this technique is a sensitive tool to evaluate treatment response in RA.

In the group of non-RA patients, three patients had ACPA-positive undifferentiated arthritis. In these patients, low numbers of TIC shape Type 4 expression were observed. Possibly these patients are ACPA-positive arthritis patients with a relatively mild form of arthritis who do not progress to RA when treated in an early phase. In our previous study in pre-clinical arthritis patients, we have shown that ACPA-positive pre-clinical RA patients do not have an increased expression of TIC Type 4 similar to healthy individuals.⁸ It might be that there is a spectrum of ACPA-positive synovitis that can develop into self-limiting arthritis and into full-blown RA.

A limitation of this study is the relatively small number of patients, especially in the RA subgroup. However, a statistically significant difference in Type 4 TIC shape was still

observed, which could not be explained by outliers. This study provides the rationale for larger studies in the future to determine the exact role of pixel-by-pixel TIC shape analysis for differential diagnosis in early RA. Furthermore, patient movement could theoretically have been a confounder, as we previously observed for wrist MRI (unpublished data). However, in this study, all patients were placed firmly in a knee coil. No significant movement was observed that influenced the data. Another limitation of our study is that we could not distinguish between venous flow and enhancing synovial tissue with the given temporal and spatial resolution in our protocol. Therefore, differences in venous flow within the ROI between the patients might perhaps be a confounding factor.

Taken together, this is the first description of DCE-MRI TIC shape analysis in early arthritis patients. Based on the association of a relatively high Type 4 TIC shape expression with RA, TIC shape analysis might be useful to differentiate between RA and non-RA patients at an early stage. Furthermore, it provides a rationale to study the relationship between TIC shape expression and development of joint destruction in a larger early RA cohort.

Rheumatology key messages

- The expression of aggressive DCE-MRI TIC shape Type 4 is increased in early RA.
- DCE-MRI TIC shape analysis might have potential as a diagnostic biomarker in early arthritis patients.

References

- 1 McQueen FM, Ostergaard M. Established rheumatoid arthritis—new imaging modalities. *Best Pract Res Clin Rheumatol* 2007;21:841-56.
- 2 Ostergaard M, Pedersen SJ, Dohn UM. Imaging in rheumatoid arthritis_status and recent advances for magnetic resonance imaging, ultrasonography, computed tomography and conventional radiography. *Best Pract Res Clin Rheumatol* 2008;22:1019-44.
- 3 Tofts PS, Brix G, Buckley DL et al. Estimating kinetic parameters from dynamic contrast-enhanced T(1)-weighted MRI of a diffusable tracer: standardized quantities and symbols. *J Magn Reson Imaging* 1999;10:223-32.
- 4 Hodgson RJ, O'Connor P, Moots R. MRI of rheumatoid arthritis image quantitation for the assessment of disease activity, progression and response to therapy. *Rheumatology* 2008;47:13-21.
- 5 Jackson A, O'Connor JP, Parker GJ et al. Imaging tumor vascular heterogeneity and angiogenesis using dynamic contrast-enhanced magnetic resonance imaging. *Clin Cancer Res* 2007;13:3449-59.
- 6 Kuhl CK, Mielcareck P, Klaschik S et al. Dynamic breast MR imaging: are signal intensity time course data useful for differential diagnosis of enhancing lesions? *Radiology* 1999;211:101-10.
- 7 Lavini C, de Jonge MC, van de Sande MG et al. Pixel-by-pixel analysis of DCE MRI curve patterns and an illustration of its application to the imaging of the musculoskeletal system. *Magn Reson Imaging* 2007;25:604-12.
- 8 van der Leij C, van de Sande MG, Lavini C et al. Rheumatoid synovial inflammation: pixel-by-pixel dynamic contrast-enhanced mr imaging time-intensity curve shape analysis - a feasibility study. *Radiology* 2009;253:234-40.
- 9 Arnett FC, Edworthy SM, Bloch DA et al. The American Rheumatism Association 1987 revised criteria for the classification of rheumatoid arthritis. *Arthritis Rheum* 1988;31:315-24.
- 10 Lavini C, Maas M. DCE-MRI analysis package comprising pixel-by-pixel classification of time intensity curves shapes, permeability maps and Gd concentration calculation. *Magn Reson Mat Phys Biol Med* 2008;21:486.
- 11 Cimmino MA, Parodi M, Innocenti S et al. Dynamic magnetic resonance of the wrist in psoriatic arthritis reveals imaging patterns similar to those of rheumatoid arthritis. *Arthritis Res Ther* 2005;7:R725-31.
- 12 Suter LG, Fraenkel L, Braithwaite RS. Role of magnetic resonance imaging in the diagnosis and prognosis of rheumatoid arthritis. *Arthritis Care Res* 2011;63:675-88.
- 13 Boyesen P, Haavardsholm EA, Ostergaard M et al. MRI in early rheumatoid arthritis: synovitis and bone marrow oedema are independent predictors of subsequent radiographic progression. *Ann Rheum Dis* 2011;70:428-33.
- 14 Duer-Jensen A, Hørslev-Petersen K, Hetland ML et al. MRI bone edema is an independent predictor of development of rheumatoid arthritis in patients with early undifferentiated arthritis. *Arthritis Rheum* 2011;63:2192-202.
- 15 Schwenzer NF, Kotter I, Henes JC et al. The role of dynamic contrast-enhanced MRI in the differential diagnosis of psoriatic and rheumatoid arthritis. *AJR Am J Roentgenol* 2010;194:715-20.
- 16 Kubassova O, Boesen M, Cimmino MA et al. A computer-aided detection system for rheumatoid arthritis MRI data interpretation and quantification of synovial activity. *Eur J Radiol* 2010;74:e67-72.
- 17 Armitage P, Behrenbruch C, Brady M et al. Extracting and visualizing physiological parameters using dynamic contrast-enhanced magnetic resonance imaging of the breast. *Med Image Anal* 2005;9:315-29.
- 18 Tak PP, Zvaifler NJ, Green DR et al. Rheumatoid arthritis and p53: how oxidative stress might alter the course of inflammatory diseases. *Immunol Today* 2000;21:78-82.
- 19 Verstraete KL, Lang P. Bone and soft tissue tumors: the role of contrast agents for MR imaging. *Eur J Radiol* 2000;34:229-46.
- 20 Hawighorst H, Libicher M, Knopp MV et al. Evaluation of angiogenesis and perfusion of bone marrow lesions: role of semiquantitative and quantitative dynamic MRI. *J Magn Reson Imaging* 1999;10:286-94.